Progress In Electromagnetics Research B, Vol. 64, 103–117, 2015

Modified π-shaped Slot Loaded Multifrequency Microstrip Antenna

Sudipta Das[1, *], Partha P. Sarkar[2], and Santosh K. Chowdhury[3]

Abstract—A single layer, single feed microstrip antenna with multifrequency operation in compact size is proposed. A modified inverted π-shaped slot is introduced at the left side radiating edge of the patch to reduce the size of the antenna by reducing the resonant frequency. Multiple resonant frequencies with increased frequency ratio are also obtained by cutting the modified inverted π-shaped slot. The measured result shows that the proposed antenna resonates at 3.3, 4.55, 5.56 and 6.08 GHz in microwave S and C band. The size of the proposed patch is only $0.176\lambda_L \times 0.132\lambda_L$ at its lower operating frequency. The proposed patch antenna has achieved 68% size reduction as compared with the conventional rectangular microstrip antenna with same patch area. An extensive analysis of the reflection coefficient, voltage standing wave ratio, gain, radiation efficiency and radiation pattern of the proposed antenna is presented in this paper. The proposed antenna is suitable for WiMax and HiPERLAN wireless systems.

1. INTRODUCTION

The rapid growth of modern wireless communication systems has increased the demand for multifrequency antennas, capable to be embedded in wireless communication devices. In recent years, the rapid decrease in size of wireless communication devices has also lead to the need for compact antennas. To support the high mobility necessity for a wireless communication device, microstrip patch antenna is likely to be preferred due to its small size, light weight, and low profile. The size of wireless communication devices can be reduced by minimizing the size of the components used inside these devices. As microstrip antenna is one of the components being used, the size of these devices depends on this antenna to a large extent. Therefore, one of the techniques of reducing the size of the wireless and handheld communication devices is to reduce the size of the microstrip antenna. A number of techniques have been reported to reduce the size of the microstrip antenna. It was reported by Kuo and Wong [1] that by embedding three meandering slots in the ground plane of rectangular microstrip patch antenna, the size of the antenna can be reduced by 56%. Rezvani et al. reported that antenna size reduction of 34% can be achieved by using slotted microstrip patch antenna with defected ground plane [2]. It was reported by Wong et al. [3] that by using shorting pin and meandered circular patch, size of the antenna can be reduced by less than 10%. Mitra and Chaudhuri reported a split ring resonator-loaded CPW-fed antenna with 26% reduction in antenna size [4]. A planar fed microstrip antenna achieved size reduction of up to 40% by inserting slots of optimum dimensions into one of the radiating edges of the patch and parallel to the non-radiating edge [5]. A maximum antenna size reduction of 41% with multifrequency operation was achieved in [6] by varying the positions and dimensions of the rectangular slots on the patch. It was also reported by Singh et al. [7] that by using cross slot on the rectangular and trapezoidal patch, the size of the antenna can be reduced by 34 and

Received 9 September 2015, Accepted 11 November 2015, Scheduled 17 November 2015

* Corresponding author: Sudipta Das (sudipta.das1985@gmail.com).

[1] Department of Electronics and Communication Engineering, IMPS College of Engineering and Technology, India. [2] Department of Engineering and Technological Studies, University of Kalyani, India. [3] Department of Electronics and Tele-Communication Engineering, Jadavpur University, India.

41%, respectively. In [8], a maximum size reduction of 46.2% was achieved by introducing a triangular slot at the upper edge of the patch. A maximum size reduction of 47.4% was reported in [9] by cutting three unequal rectangular slots at the edge of the patch. It was reported by Malekpoor and Jam [10] that by cutting the different slots length on the patch and using unequal resonance arms, the size of the microstrip patch antenna can be reduced by 37% with multi-frequency operation. Kaya et al. designed and studied rectangular microstrip antenna with a pair of parallel slots loaded close to the radiating edge of the patch and three meandering narrow slots embedded in the antenna surface resulted in a size reduction of 34 and 45% [11]. Antenna size reduction of about 61% with multifrequency operation was reported in [12]. A maximum size reduction of less than 40% was reported in [13] for slotted edge fed microstrip antenna. A compact equilateral triangular patch antenna with maximum size reduction of 43.47% was reported in [14]. Recently, Das et al. has designed a monitor-shaped multifrequency microstrip patch antenna with 66% reduction in antenna size [15]. A maximum antenna size reduction of about 50% was reported in [16] by means of inductive slots. Gautam et al. reported 39% size reduction by inserting four slits on the radiating square patch [17]. A meander type slot antenna fed by a stripline has achieved 56% size reduction [18]. It was reported by Song and Woo [19] that 43.9% miniaturization of microstrip patch antenna is possible by using perturbation of radiating slot. A printed microstrip window antenna with 50% size reduction was reported in [20]. A probe-fed microstrip antenna results in 51% reduction in antenna size by etching out a symmetric pattern of crossed slots from the surface of the patch [21]. The work presented in this paper relates to miniaturized multifrequency microstrip patch antenna. Our aim is to reduce the antenna size and also to achieve multiple resonant frequencies only by modifying the patch. With the introduction of modified inverted π-shaped slot on the patch, multiple resonant frequencies are obtained, and also the size of the proposed antenna has been reduced by 68% in comparison to conventional rectangular microstrip antenna with same patch area.

The novelty and advantages of the proposed antenna are as follows:

i) **Antenna Feed Position:**
The feed position of the proposed antenna remains same as conventional reference antenna. The antenna performance is parametrically optimized by introducing various slots.

ii) **Improved Gain:**
The gain of the proposed antenna is improved by obtaining good impedance matching due to the addition of small rectangular notches with the π shaped slot.

iii) **Compact Dimension:**
The proposed antenna offers multifrequency operation in much compact size without using slotted ground plane, shorting pin, artificial substrate or modifications in the feed. The radiating patch area ($16 \times 12\,\text{mm}^2$) of the proposed antenna is much less with respect to reference works [1–21] included in the literature.

iv) **Better Size Reduction:**
The antenna proposed in this article has achieved better size reduction (68%) with simple structure in comparisons to reference works [1–21].

The proposed multifrequency antenna could be promising for a number of modern wireless communication systems due to its small size, light weight, and good working characteristics. Mainly it is developed for 3.3/5.5 GHz WiMAX and 5.5 GHz HiPERLAN. The proposed antenna may be useful for radar application.

2. ANTENNA DESIGN

The configuration of the conventional antenna is given in Figure 1. The dielectric material selected for this design is an FR4 epoxy with dielectric constant (ε_r) = 4.4 and substrate height (h) = 1.5875 mm. The length and width of Antenna 1 (conventional antenna) operating at 5.5 GHz are 12 and 16 mm, respectively. The width and length of the conventional patch antenna in terms of wavelength are $0.293\lambda_r$ and $0.22\lambda_r$, respectively, where, λ_r is the wavelength of the resonant frequency (i.e., 5.5 GHz). The coaxial probe-feed of radius 0.5 mm with a simple ground plane arrangement is located at a position $W/2$ (8 mm) and $L/3$ (4 mm) from right side edge of the patch for best impedance matching.

Figure 2 shows the configuration of antenna 2 (proposed antenna) which is designed with a similar substrate. This antenna is also a 16 mm × 12 mm rectangular patch. An inverted π-shaped slot is introduced at the left side edge of the patch to reduce the size of the antenna and also to obtain multiple frequencies from the antenna. The inverted π-shaped slot is modified by cutting small rectangular notches with the arms of the π-shaped slot. The addition of rectangular notches improves the gain and reflection coefficient of the proposed antenna at multiple resonant frequencies. The coaxial probe feeding location of the proposed antenna is similar to the conventional antenna. The coaxial probe feeding point of the proposed antenna is also located at $W/2$ (8 mm) and $L/3$ (4 mm) position from the right-side edge of the patch to achieve multiple frequencies with best impedance matching. With the proposed antenna structure, alteration of location of the feed point results in less sharp resonances and poor impedance matching at the respective frequencies. The method of moment based electromagnetic simulator IE3D [22] is applied for numerical investigation in the proposed antenna design. The dimensions of the proposed antenna parameters are optimized by parametric study to meet the design goal. The optimal dimension values of the proposed antenna are given as: $L = 12$ mm, $W = 16$ mm, $L_3 = W_3 = W_4 = 1$ mm, $L_4 = W_1 = W_2 = 6$ mm, $L_5 = L_6 = L_7 = L_8 = L_9 = W_5 = 0.5$ mm.

The prototypes of the fabricated conventional and proposed antenna are shown in Figures 3–4.

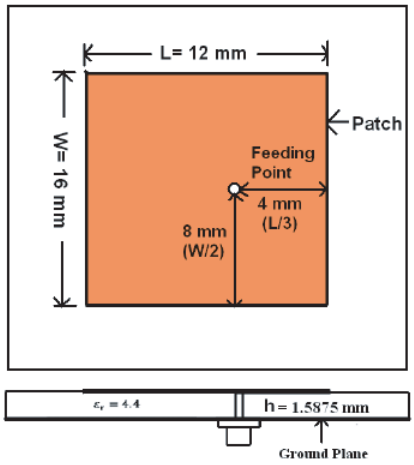

Figure 1. Configuration of Antenna 1 (Conventional antenna).

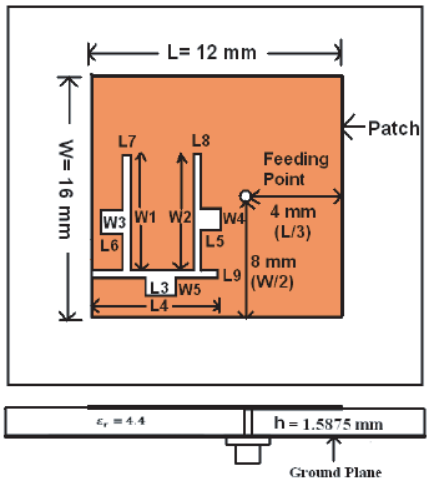

Figure 2. Configuration of Antenna 2 (Proposed antenna).

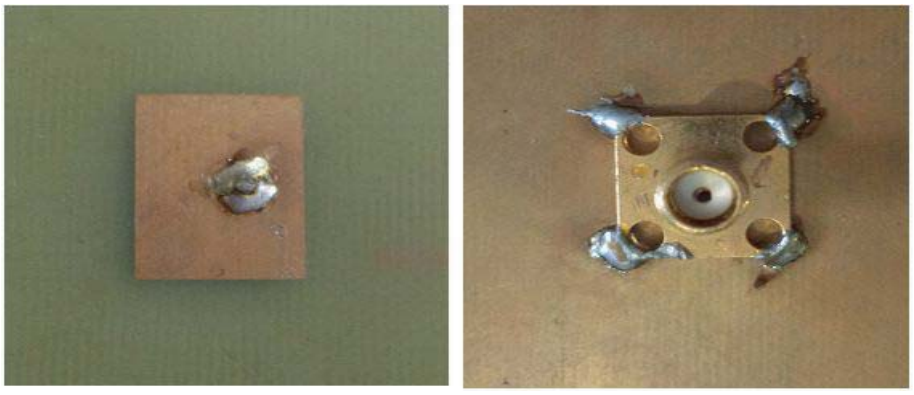

(a) (b)

Figure 3. Photograph of fabricated prototype of the conventional antenna (a) patch, (b) ground plane.

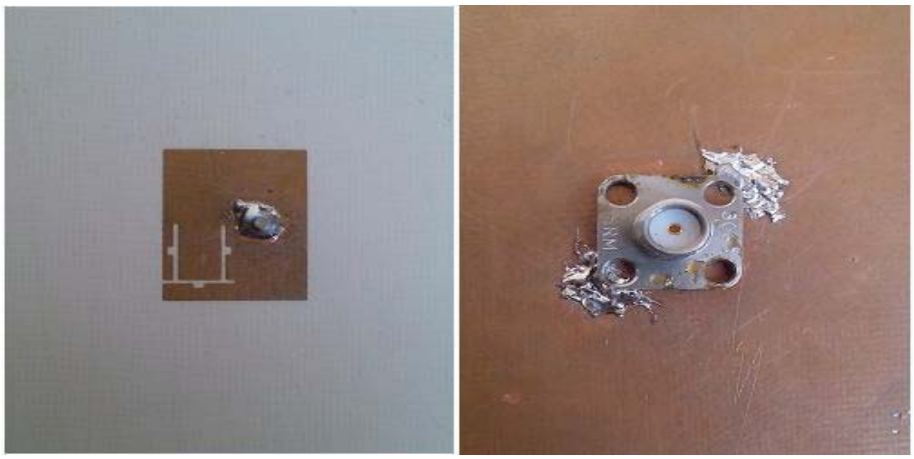

(a) (b)

Figure 4. Photograph of fabricated prototype of the proposed antenna (a) patch, (b) ground plane.

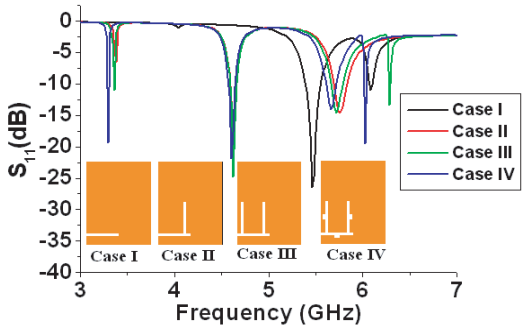

Figure 5. S_{11} variations of the antenna in different cases.

3. ANALYSIS AND WORKING OF ANTENNA 2 (PROPOSED ANTENNA)

The effect of each optimized slot on the resonant frequency of the proposed antenna is analyzed using IE3D software. Figure 5 shows the different cases of evolution of the proposed antenna and corresponding simulated reflection coefficient.

The geometry of the proposed antenna is formed from four different stages of modifications. The conventional antenna (antenna without slots) resonates at 5.5 GHz. But the resonance characteristics of the antenna changes drastically due to incorporation of slots.

For the case of only having single optimized horizontal slot in patch, fundamental mode is excited at 5.5 GHz and a second higher order resonant mode at 6.08 GHz is also emerged. It is seen from case II of Figure 5 that with the incorporation of first vertical slot, the antenna resonates at two different frequencies 4.62 and 5.76 GHz with S_{11} below -10 dB. Another resonance is observed at 3.38 GHz but impedance matching is very poor and reflection coefficient is only -6.57 dB. In case III, the additional vertical slot (forming inverted π-shape) further shifts the first resonant frequency to 3.36 GHz with improved reflection coefficient of -11 dB. The second resonant frequency remains same (i.e., 4.62 GHz) with better reflection coefficient. The third resonant frequency is slightly shifted to 5.72 GHz and a new higher order resonant frequency is excited at 6.28 GHz. Finally in case IV (proposed), the structure is modified by inserting small rectangular slots at middle of every resonance arm of inverted π-shaped slot. Now, the proposed antenna resonates at 3.3, 4.6, 5.66 and 6.02 GHz with much better reflection coefficients.

The proposed antenna with this modified inverted π-shaped slot provides three advantages:

i) The lower resonant frequency is further reduced. This offers better compactness. The width and

length of the proposed antenna in terms of wavelength at the lower resonant frequency are $0.176\lambda_L$ and $0.132\lambda_L$, respectively.

ii) Better impedance matching is achieved at respective frequencies due to improvement of reflection coefficient and VSWR.

iii) The gain of the antenna also improves at respective frequencies. The gain of the antenna is improved by obtaining good impedance matching. So, due to better impedance matching, antenna efficiency increases which improves the gain of the antenna.

The variations of resonant frequency, reflection coefficient, gain, and VSWR in different cases of evolution of proposed antenna are summarized below in Table 1.

Table 1. Variations of simulated results in different cases of evolution of proposed antenna.

Different Cases	Resonant Frequency (GHz)	S_{11} (dB)	Gain (dBi)	VSWR	Size Reduction (%)
Case I	$f_1 = 5.5$	-26.5	5.25	1.099	0
	$f_2 = 6.08$	-11	3.4	1.78	
Case II	$f_1 = 3.38$	-6.57	3.3	2.766	35
	$f_2 = 4.62$	-23.2	4.05	1.148	
	$f_3 = 5.76$	-14.6	5.02	1.456	
Case III	$f_1 = 3.36$	-11	3.93	1.78	66
	$f_2 = 4.62$	-24.7	4.95	1.122	
	$f_3 = 5.72$	-14.6	4.02	1.456	
	$f_4 = 6.28$	-13.4	2.45	1.543	
Case IV (Proposed)	$f_1 = 3.3$	-19.4	4.25	1.239	68
	$f_2 = 4.6$	-21.8	5.25	1.176	
	$f_3 = 5.66$	-14	5.15	1.497	
	$f_4 = 6.02$	-19.5	4.15	1.236	

4. PARAMETRIC STUDY OF THE PROPOSED ANTENNA

4.1. Effect of Antenna Parameter L_4

The effects of varying the dimensions of the slots on the resonant characteristics of the proposed antenna are investigated by parametric study. The effective parameters are investigated by simulating the antenna with one geometry parameter slightly changed from the reference design while all the other parameters are fixed. All the parametric studies are performed through simulations without altering the feeding location of the antenna.

The variations of reflection coefficient and resonant frequency of the proposed antenna as a function of design parameter L_4 is shown in Figure 6. With the increase of L_4 than proposed dimension, the first resonant frequency is further shifted to 3.08 GHz and that is due to the fact that the current path at this frequency increases. But the value of reflection coefficient at 3.08 GHz decreases to -8 dB due to impedance mismatching. The value of S_{11} should be at least -10 dB, which is the main criterion for an antenna to radiate in the far field region. The second resonant frequency remains unchanged with the variations of parameter L_4. The third and fourth resonant frequency can be easily tuned by adjusting the value of the design parameter L_4.

4.2. Effect of Antenna Parameter W_1

The impact of design parameter W_1 is shown in Figure 7. It is clearly seen that further increase of W_1 compared with proposed dimension will slightly shift the first resonant frequency with different

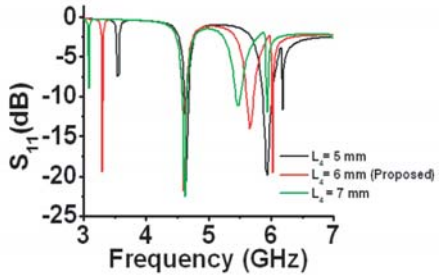

Figure 6. S_{11} variations for different values of L_4.

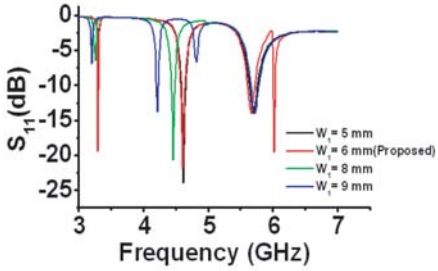

Figure 7. S_{11} variations for different values of W_1.

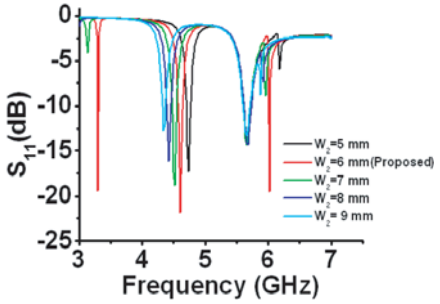

Figure 8. S_{11} variations for different values of W_2.

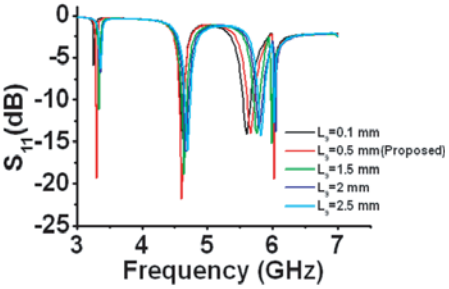

Figure 9. S_{11} variations for different values of L_9.

impedance matching. The tuning of the second resonant frequency is possible by increasing the value of W_1 parameter. When the value of W_1 increases to 9 mm, a new resonant mode is excited at 4.82 GHz, but S_{11} is only -6.67 dB, which indicates poor impedance matching. The third frequency band remains stationary with the variation of W_1 slot parameter. The excitation of fourth resonant frequency is possible only with the proposed value of W_1 parameter. So, an optimum value of $W_1 = 6$ mm is selected for antenna design. The generation of fourth resonant frequency is not possible with further change in W_1 parameter.

4.3. Effect of Antenna Parameter W_2

Similarly, according to Figure 8, when the values of slot parameter W_2 increases to 7 mm, the first resonant frequency is decreased to 3.14 GHz with S_{11} of only -4 dB, which suggests poor impedance matching. The excitation of first resonant frequency is not possible with further increase in W_2 parameter of the proposed antenna. So, an optimum value of $W_2 = 6$ mm is selected as a slot parameter for antenna design. The second frequency band is tuned by increasing or decreasing the dimension of the slot. The third frequency band remains unaltered with the variation of W_2 parameter. It is observed that shifting of fourth resonant frequency depends inversely on dimension of W_2 parameter of the antenna. But maximum reflection coefficient i.e., best impedance matching is achieved for $W_2 = 6$ mm.

4.4. Effect of Antenna Parameter L_9

Figure 9 illustrates variations of S_{11} curve versus variation of the parameter L_9. For example, when L_9 varies from 0.1 mm to 2.5 mm, the resonant frequency of the second mode moves from 4.6 GHz to 4.7 GHz. The parameter L_9 has great impact on resonant frequency of the third mode. The resonant mode for 5.66 GHz can be tuned from 5.6 GHz to 5.84 GHz by adjusting the dimension of 'L_9' parameter from 0.1 mm to 2.5 mm. The maximum reflection coefficients for the first and fourth resonant mode is achieved due to proposed dimension of $L_9 = 0.5$ mm. So, an optimum value of 0.5 mm is selected for L_9 to achieve an optimal design of the proposed antenna.

4.5. Effect of Antenna Parameter L_7

Simulated S_{11} curves for different values of L_7 are illustrated in Figure 10. It is seen from the figure that increasing the slot length L_7 than proposed dimension leads to shift of fourth resonant mode at 6.02 GHz towards the third resonant mode, thus decreasing the frequency ratio between third and fourth resonant frequency. Simultaneously, it has little impact on second resonant mode. Also the first and third resonant frequencies appear with different impedance matching due to change in dimension of L_7 parameter. So, it is clear from Figure 10 that $L_7 = 0.5$ mm is the optimum value for the proposed antenna to achieve multifrequency operation with best impedance matching.

4.6. Effect of Antenna Parameter L_8

Figure 11 shows the variation on the reflection coefficient with parameter L_8. It can be observed that with increasing the slot width up to $L_8 = 1.5$ mm, both first and second resonant frequencies slightly shift downwards. Again, with decreasing the slot width, both resonant frequencies shift upward. The third resonant mode remains almost same. The fourth resonant mode at 6.02 GHz appears with poor impedance matching due to further increase in dimension of 'L_8' parameter compared with proposed dimension. The best impedance matching with multifrequency operation is achieved for the proposed slot dimension. Thus, slot dimension, L_8, equal to 0.5 mm is used as the optimized value.

4.7. Effect of First Rectangular Notch Depth W_5

Figure 12 illustrates the S_{11} for different values of notch depth W_5. It is observed that impedance matching of the first resonant mode at 3.3 GHz is greatly influenced by the change in W_5 parameter of the proposed antenna. The best impedance matching at first resonant mode is achieved for $W_5 = 0.5$ mm. The third resonant frequency can be tuned downward with similar impedance matching by increasing

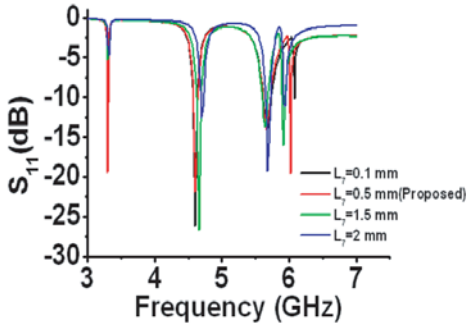

Figure 10. S_{11} variations for different values of L_7.

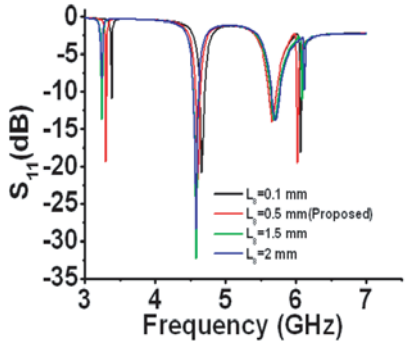

Figure 11. S_{11} variations for different values of L_8.

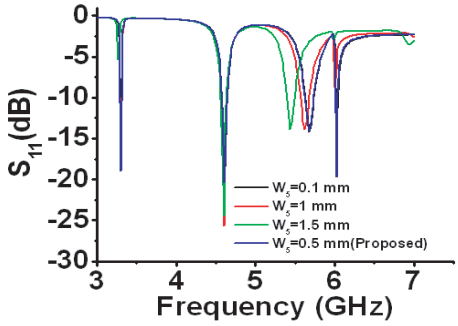

Figure 12. S_{11} variations for different values of W_5.

the dimension of W_5 parameter. The excitement of fourth resonant mode is not possible when W_5 parameter equals to 1.5 mm. An optimum value of $W_5 = 0.5$ mm is selected for the antenna design.

4.8. Effect of Second Rectangular Notch Depth L_5

The first resonant mode at 3.3 GHz is greatly influenced by the variations in notch depth L_5. It is seen from Figure 13 that increasing the notch depth L_5 leads to the shift towards the lower frequencies of resonant mode at 3.18 GHz but impedance matching becomes very poor. The second and third resonant frequency appears stationary but the impedance matching at fourth resonant frequency degrades due to increase in dimension of L_5 parameter. So, an optimum value of 0.5 mm is selected for the proposed antenna.

4.9. Effect of Third Rectangular Notch Depth L_6

In Figure 14, the variation of notch depth L_6 is shown. It can be observed that fourth resonant mode is highly affected and shift downward with increasing dimension of L_6 parameter. If $L_6 = 0.7$ mm, the performance of the antenna is degrading because fourth band comes much closer to the third band which may increase the cross polarization level of the antenna. Also, S_{11} for first resonant mode decreases for $L_6 = 0.7$ mm. Again, $L_6 = 0.1$ mm dimension is practically not realizable because 0.3 mm dimension is the minimum requirement for the fabrication purpose. Thus, $L_6 = 0.5$ mm is the proposed dimension for the antenna design.

4.10. Effect of Rectangular Notch Widths L_3, W_3 and W_4 on the Performance of the Proposed Antenna

The S_{11} variations of the proposed antenna for different values of notch widths are shown in Figures 15–17. It is observed from the figures that further frequency shifting is not possible by changing the

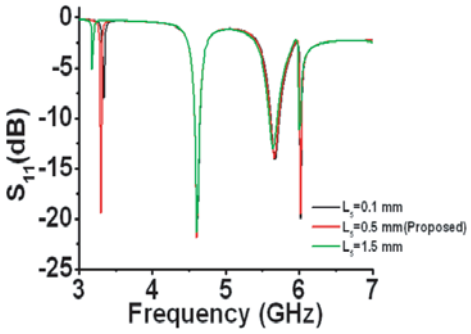

Figure 13. S_{11} variations for different values of L_5.

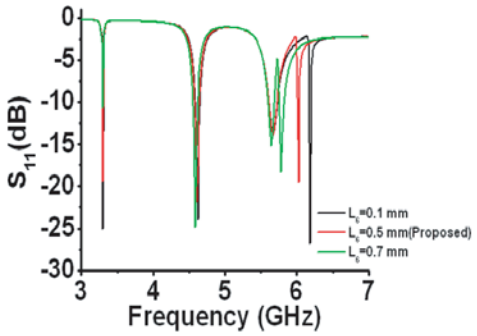

Figure 14. S_{11} variations for different values of L_6.

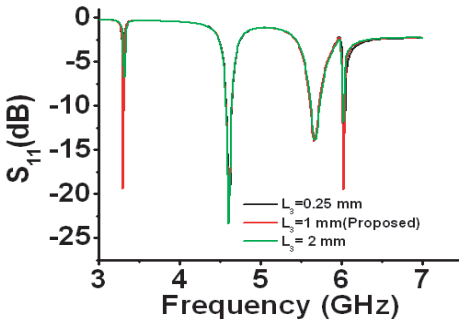

Figure 15. S_{11} variations for different values of L_3.

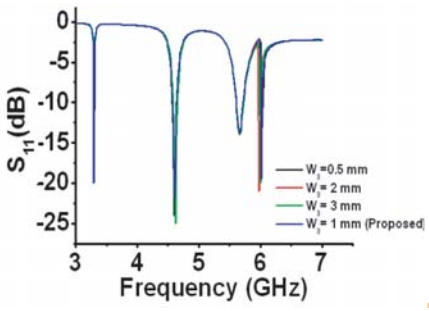

Figure 16. S_{11} variations for different values of W_3.

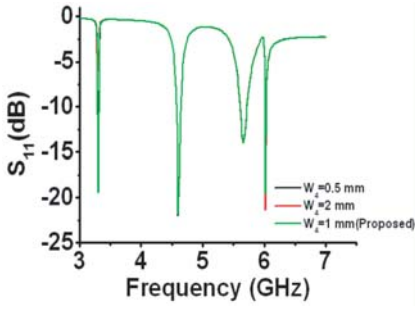

Figure 17. S_{11} variations for different values of W_4.

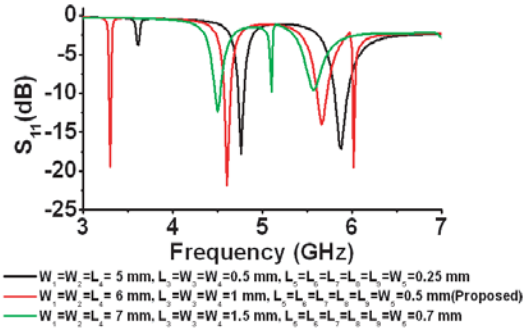

Figure 18. S_{11} vs. frequency as a function of modified inverted π-shaped slot parameters.

Table 2. Simulated results of the proposed antenna by varying the dimensions of modified inverted π-shaped slot.

Slot dimensions (mm)	**Frequency (GHz)**	S_{11} **(dB)**	**Frequency Ratio**	**Size Reduction (%)**
$W_1 = W_2 = L_4 = 5$, $L_3 = W_3 = W_4 = 0.5$, $L_5 = L_6 = L_7 = L_8 = L_9 = W_5 = 0.25$	$f_1 = 4.76$, $f_2 = 5.88$	-17.83, -17.17	$\frac{f_2}{f_1} = 1.235$	31
$W_1 = W_2 = L_4 = 6$, $L_3 = W_3 = W_4 = 1$, $L_5 = L_6 = L_7 = L_8 = L_9 = W_5 = 0.5$ **(Proposed)**	$f_1 = 3.3$, $f_2 = 4.6$, $f_3 = 5.66$, $f_4 = 6.02$	-19.4, -21.8, -14, -19.5	$\frac{f_2}{f_1} = 1.393$ $\frac{f_3}{f_1} = 1.715$ $\frac{f_4}{f_1} = 1.824$	68
$W_1 = W_2 = L_4 = 7$, $L_3 = W_3 = W_4 = 1.5$, $L_5 = L_6 = L_7 = L_8 = L_9 = W_5 = 0.7$	$f_1 = 4.5$, $f_2 = 5.1$, $f_3 = 5.56$	-12.37, -9.83, -9.58	$\frac{f_2}{f_1} = 1.133$ $\frac{f_3}{f_1} = 1.235$	38

dimension of the notch widths. But the values of S_{11} parameter changes due to variations in notch widths. Furthermore, good impedance matching is obtained for the proposed dimensions, which is found in the respective S_{11} graphs.

The effect of change in all the design parameters at the same time on the resonant frequency of the proposed antenna is shown in Figure 18. The results of Figure 18 are summarized in Table 2. It is notable that with the decrease in slot dimensions, the antenna resonates at dual frequency with

only 31% compactness. Similarly, according to Table 2, when the slot dimension increases, the antenna provides triple frequency operation with only 38% reduction in size. But it is interesting to note from Table 2 that maximum frequency ratio remains same in both of the cases. The antenna offers 68% size reduction and multiple frequencies with frequency ratio varying in between 1.393 to 1.824, when designed with proposed slot dimensions. The excitation of first resonant frequency (i.e., 3.3 GHz) is possible only when the antenna is designed with proposed slot dimensions. It can be concluded from results mentioned in Table 2 that the antenna offers multiple resonant frequencies, improved reflection coefficient, increased frequency ratio and better size reduction, when designed with proposed slot dimensions. So, the proposed antenna dimensions are optimum to achieve multifrequency operation with good impedance matching in compact size.

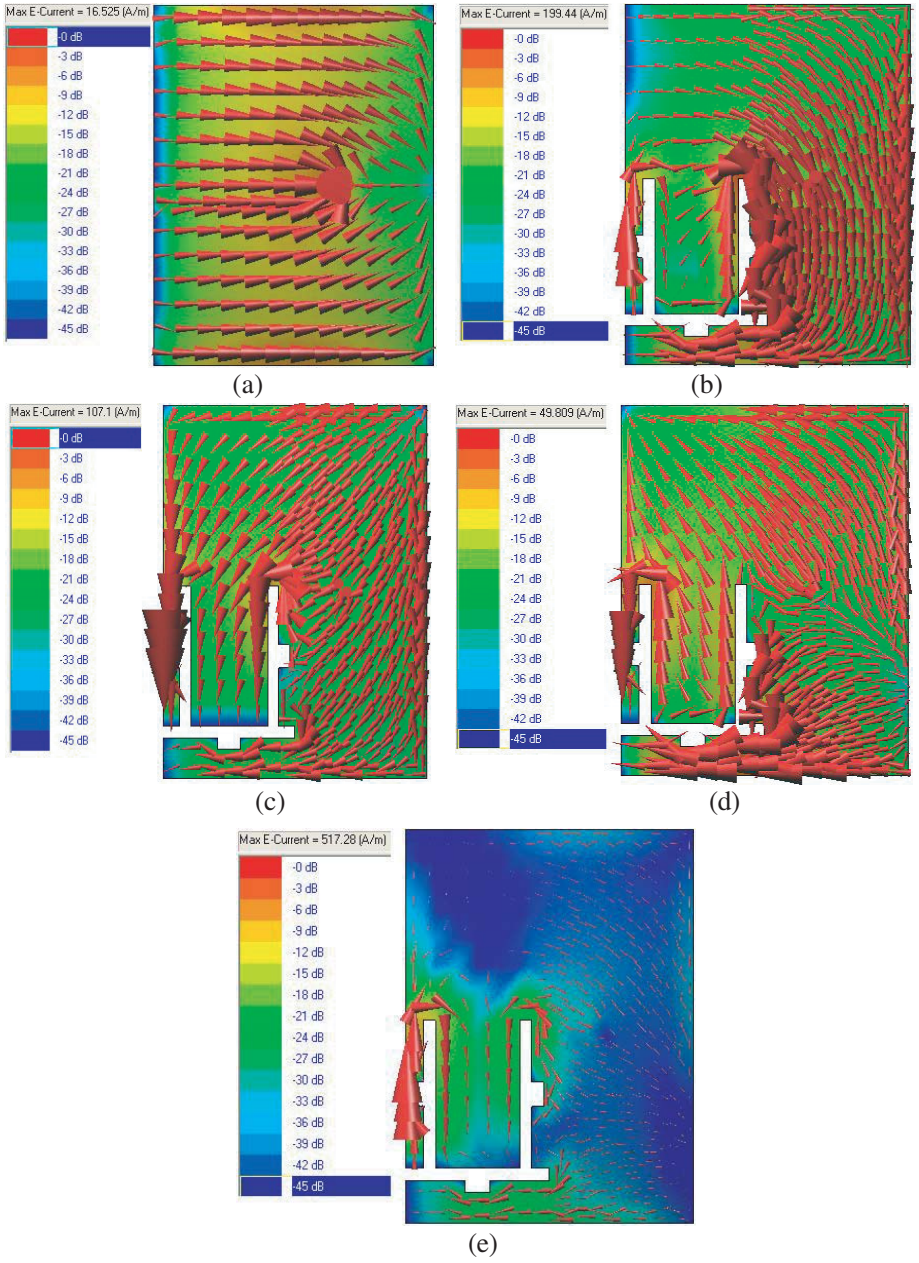

Figure 19. Surface current distribution of Antenna 1 (Conventional) at (a) 5.5 GHz and Antenna 2 (Proposed) at (b) 3.3 GHz, (c) 4.6 GHz, (d) 5.66 GHz, (e) 6.02 GHz.

5. SURFACE CURRENT DISTRIBUTION OF CONVENTIONAL AND PROPOSED ANTENNA

For better understanding the excitation behavior of the conventional and proposed antenna, surface current distributions for different resonant frequencies are studied and displayed in Figures 19(a)–19(e). It is clearly observed from Figure 19(a) that the surface current density is much less at the left side radiating edge of the conventional patch. So, the current density of the patch at that radiating edge can be increased by introducing additional slots [23]. Because of the presence of modified inverted π-shaped slot at the left side edge of the patch, there is a change in the surface current density. It is clearly seen from Figure 19(b) that for 3.3 GHz operation, the surface current is largely concentrated around both horizontal and vertical arms of the modified π-shaped slot for which it is generated. For the 4.6 GHz excitation [see Figure 19(c)], large surface current distribution is observed along the vertical slotted arms of the π-shaped slot. As depicted in Figure 19(d), for third resonant mode at 5.66 GHz, strong current distribution is observed on the horizontal slot parameters and along one vertical slot for which this resonance mode is generated and controlled. Finally, it is verified from Figure 19(e) that for fourth resonant mode at 6.02 GHz, surface current density is much stronger around one of the vertical arm (W_1, L_7, W_3, and L_6) of the modified inverted π-shaped slot. Thus, both from the S_{11} characteristic curves and surface current distributions, we can clearly comprehend the function of the related geometrical mechanism of the proposed antenna at four resonant modes. The modified inverted π-shaped slot is loaded into the patch in such a way so that the number of resonant frequency increases due to the disturbance caused to the mean current paths of any resonant mode. This is due to the fact that when the slots are cut along the radiating edge and surface of the rectangular patch, the electric and magnetic field distribution changes due to the lengthening of the surface current around the slots. The current mainly concentrates at edges of the slot and thereby increases the current path. Due to the lengthening of the surface current around the slot, the resonant frequency decreases which leads to miniaturization of the proposed antenna.

6. RESULTS AND DISCUSSION

The prototypes of Antenna 1 (conventional) and Antenna 2 (proposed antenna, with modified inverted π-shaped slot) were fabricated and tested. The reflection coefficient and VSWR were measured using Agilent E5071B vector network analyzer. The simulated and measured reflection coefficients of Antenna 1 (conventional antenna) are shown in Figure 20. The comparison of the measured S_{11} with the simulated ones of Antenna 2 is shown in Figure 21. The small discrepancy between the measured and simulated result is due to the effect of improper soldering of SMA connector or fabrication tolerance. In comparison with a conventional patch antenna, 68% size reduction is achieved by the proposed structure. The measured VSWR and mismatch loss of the proposed antenna is shown in Figure 22. The VSWR of the proposed antenna are within 2 : 1 which signifies less reflected power and practically considerable mismatch loss throughout different resonant frequencies. The simulated gain and radiation efficiency of the proposed antenna is depicted in Figure 23.

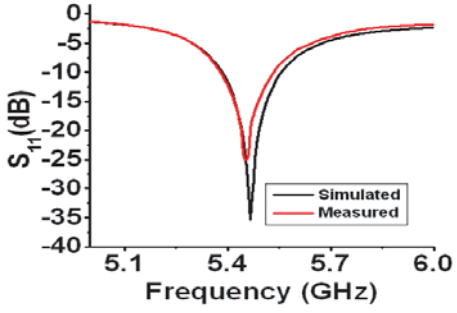

Figure 20. Reflection coefficient of Antenna 1 (Conventional Antenna).

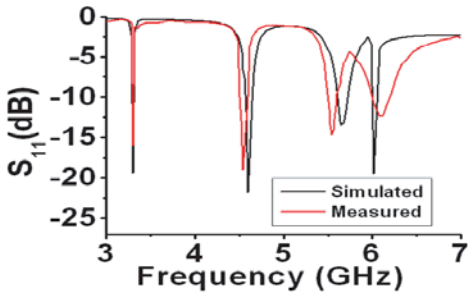

Figure 21. Reflection coefficient of Antenna 2 (Proposed Antenna).

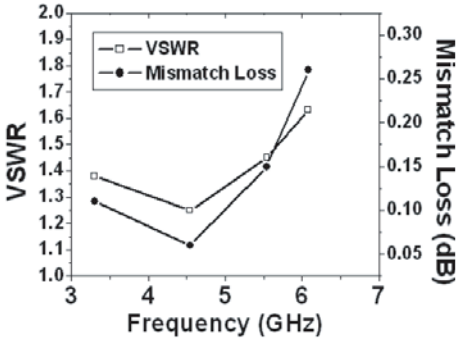

Figure 22. Measured VSWR and Mismatch loss.

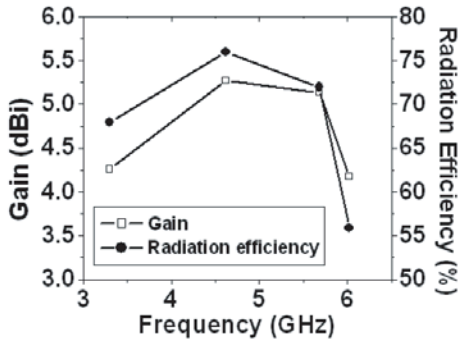

Figure 23. Plot of Gain and radiation efficiency.

6.1. Calculation of Mismatch Loss (ML)

The mismatch loss (ML) is calculated from the measured VSWR using the following expression

$$ML = -10\log\left\{1 - \left[\frac{VSWR-1}{VSWR+1}\right]^2\right\} \tag{1}$$

The simulated gain of the proposed antenna lies above 4.15 dBi for all the resonant frequencies (3.3, 4.6, 5.66 and 6.02 GHz). Simulated peak gain of about 5.25 dBi is achieved at 4.6 GHz. The measured peak gain of about 5.7 dBi is achieved at 4.55 GHz. It is found that for lower frequency of operation, the radiation efficiency of the antenna is about 68%. Peak radiation efficiency of about 77% is achieved at 4.6 GHz. Figure 24 shows the simulated input impedance loci of 48.84 + j0.123 at 3.3 GHz, 45.05 + j1.70 at 4.6 GHz, 50.19 − j20.44 at 5.66 GHz and 44.56 + j1.37 at 6.02 GHz with four loops in smith chart justifying that the proposed patch design offered fine and steady impedance matching between the feed and the antenna in the quad operating band.

The simulated and measured normalized E plane radiation patterns of proposed antenna are shown in Figure 25. Maximum radiation is exactly concentrated along 0°. It can be observed from the radiation patterns that there is almost stable response throughout different resonant frequencies. The slight noted asymmetry between the measured and simulated radiation pattern is due to feed which is not symmetrically positioned along the E-plane. The radiation patterns may also differ due to tolerance in measurement process or unavailability of anechoic chamber for measurement. The measured results of Antenna 1 and Antenna 2 are summarized in Table 3.

Table 3. Measured results of the conventional antenna and proposed antenna.

Antenna	Resonant freq. (GHz)	S_{11} (dB)	−10 dB Band width (MHz)	Gain (dBi)	Frequency ratio
Conventional Antenna	5.45	−23	150	5.4	
Proposed Antenna	$f_1 = 3.3$ $f_2 = 4.55$ $f_3 = 5.56$ $f_4 = 6.08$	−16 −19 −14.7 −12.4	40 100 110 210	4.5 5.7 5.5 4.3	$f_2/f_1 = 1.378$ $f_3/f_1 = 1.684$ $f_4/f_1 = 1.842$

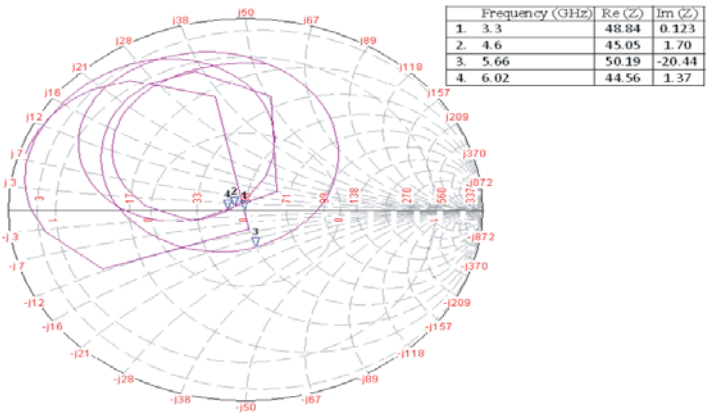

Figure 24. Input impedance loci of proposed antenna.

Table 4. Performance comparison of the proposed antenna with other reference works.

Works	Size reduction (%)	Maximum Gain (dBi)	Maximum operating bandwidth (MHz)
Ref. [1]	56	3.9	50
Ref. [2]	34	2.2	210
Ref .[4]	26	1.9	200
Ref. [5]	40	4.2	100
Ref. [6]	41	5.0	360
Ref. [8]	46.2	5.37	160
Ref. [9]	47.4	5.44	202
Ref. [10]	37	7.7	130
Ref. [12]	61	5.25	140
Ref. [14]	43.47	4.99	57
Ref. [15]	66	5.4	120
Ref. [19]	43.9	4.3	85
Ref. [20]	50	3.7	100
Ref. [21]	51	0.9	10
This paper	68	5.7	210

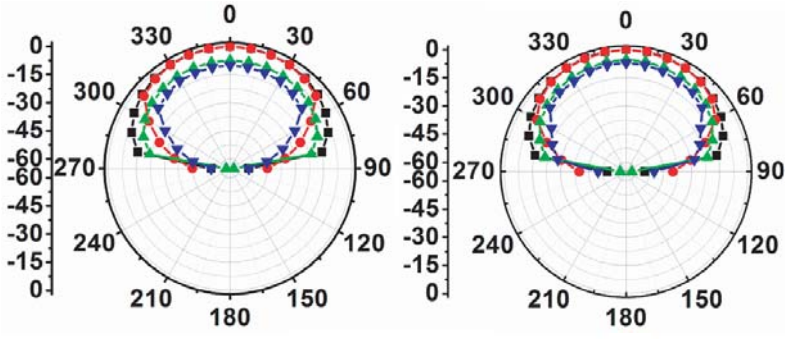

(a) (b)

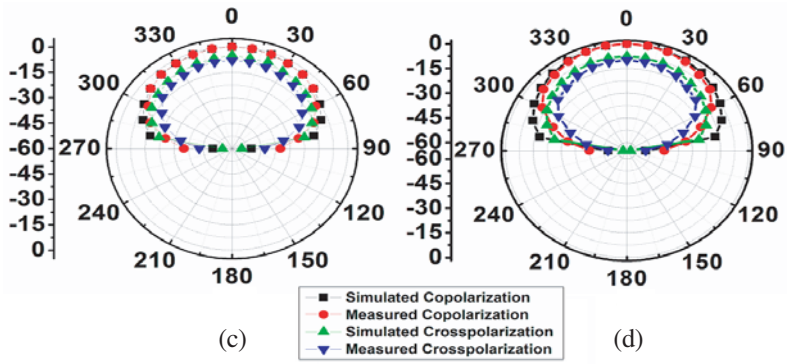

Figure 25. Simulated and Measured normalized E plane radiation pattern of the proposed antenna at (a) 3.3 GHz (b) 4.55 GHz (c) 5.56 GHz (d) 6.08 GHz.

7. PERFORMANCE COMPARISON OF THE PROPOSED ANTENNA WITH SOME REFERENCE WORKS

The performance comparison (size reduction, gain and bandwidth) of the proposed antenna with some other miniaturized antennas is shown in Table 4.

8. CONCLUSION

A novel compact modified inverted π-shaped slot loaded microstrip antenna with multifrequency operation is presented and investigated. An optimization between miniaturization and impedance matching is maintained in this work. The proposed antenna offers 68% size reduction with increased frequency ratio and multi-frequency operation. Furthermore, good stable radiation patterns and acceptable gain are also obtained across the operating frequencies. The measured 3 dB beam-width of radiation patterns for the proposed antenna varies 68 and 80°, which are acceptable because it is intended. The proposed antenna can be promising and suitable for 3.3/5.5 GHz WiMAX and 5.5 GHz HiPERLAN.

REFERENCES

1. Kuo, J. S. and K. L. Wong, "A compact microstrip antenna with meandering slots in the ground plane," *Microwave Opt. Technol. Lett.*, Vol. 29, 95–97, 2001.
2. Rezvani, S., Z. Atlasbaf, and K. Forooraghi, "A novel miniaturized reconfigurable slotted microstrip patch antenna with defected ground structure," *Electromagn.*, Vol. 31, 349–354, 2011.
3. Wong, K.-L., C.-L. Tang, and H.-T. Chen, "A compact meandered circular microstrip antenna with a shorting pin," *Microwave Opt. Technol. Lett.*, Vol. 15, 147–149, 1997.
4. Mitra, D. and S. R. B. Chaudhuri, "CPW-fed miniaturized split ring-loaded slot antenna," *Microwave Opt. Technol. Lett.*, Vol. 54, 1907–1911, 2012.
5. Elsdon, M., A. Sambell, and Y. Qin, "Reduced size direct planar-fed patch antenna," *Electronics Letters*, Vol. 41, 884–886, 2005.
6. Bhunia, S., M. K. Pain, S. Biswas, D. Sarkar, P. P. Sarkar, and B. Gupta, "Investigations on microstrip patch antennas with different slots and feeding points," *Microwave Opt. Technol. Lett.*, Vol. 50, 2754–2758, 2008.
7. Singh, L. L. K., B. Gupta, P. P. Sarkar, K. Yoshitomi, and K. Yasumoto, "Cross slot multi frequency patch antenna," *Microwave Opt. Technol. Lett.*, Vol. 53, 611–615, 2011.
8. Chakraborty, U., S. Chatterjee, S. K. Chowdhury, and P. P. Sarkar, "A compact microstrip patch antenna for wireless communication," *Progress In Electromagnetics Research C*, Vol. 18, 211–220, 2010.

9. Chatterjee, S., S. K. Chowdhury, P. P. Sarkar, and D. C. Sarkar, "Compact microstrip patch antenna for microwave communication," *Indian J. Pure Appl. Phys.*, Vol. 51, 800–807, 2013.
10. Malekpoor, H. and S. Jam, "Design of a multiband asymmetric patch antenna for wireless applications," *Microwave Opt. Technol. Lett.*, Vol. 55, 730–734, 2013.
11. Kaya, A., "Meandered slot and slit loaded compact microstrip antenna with integrated impedance tuning network," *Progress In Electromagnetics Research B*, Vol. 1, 219–235, 2008.
12. Das, S., A. Karmakar, P. P. Sarkar, and S. K. Chowdhury, "Design and analysis of a novel open ended T-shaped slot loaded compact multifrequency microstrip patch antenna," *Microwave Opt. Technol. Lett.*, Vol. 56, 316–322, 2014.
13. Park, Z. and C.-H. Cho, "Size reduction and multiresonance effects of slotted single layer edge-fed patch antennas," *J. Korean Phys. Soc.*, Vol. 61, 623–625, 2012.
14. Dasgupta, S., B. Gupta, and H. Saha, "Compact equilateral triangular patch antenna with slot loading," *Microwave Opt. Technol. Lett.*, Vol. 56, 268–274, 2014.
15. Das, S., P. P. Sarkar, and S. K. Chowdhury, "Design and analysis of a compact monitor-shaped multifrequency microstrip patch antenna," *Journal of Electromagnetic Waves and Applications*, Vol. 28, No. 7, 827–837, 2014.
16. Reed, S, L. Desclos, C. Teret, and S. Toutain, "Patch antenna size reduction by means of inductive slots," *Microwave Opt. Technol. Lett.*, Vol. 29, 79–81, 2001.
17. Gautam, A. K., P. Benjwal, and B. K. Kanaujia, "A compact square microstrip antenna for circular polarization," *Microwave Opt. Technol. Lett.*, Vol. 54, 897–900, 2012.
18. Kim, J.-M., K.-W. Kim, J.-G. Yook, and H.-K. Park, "Compact stripline-fed meander slot antenna," *Electronics Lett.*, Vol. 37, 995–996, 2001.
19. Song, M.-H. and J.-M. Woo, "Miniaturization of microstrip patch antenna using perturbation of radiating slot," *Electronics Lett.*, Vol. 39, 417–419, 2003.
20. Xue, Q., K. M. Shum, C. H. Chan, and K. M. Luk, "A novel printed microstrip window antenna for size reduction and circuit embedding," *Microwave Opt. Technol. Lett.*, Vol. 32, 192–194, 2002.
21. Gosalia, K. and G. Lazzi, "Reduced size, dual-polarized microstrip patch antenna for wireless communications," *IEEE Trans. on Antennas and Propagation*, Vol. 51, 2182–2186, 2003.
22. Zeland Software Inc., "IE3D: MoM-based EM simulator," Zeland Software Inc., Fremont, CA.
23. Das, S., P. P. Sarkar, and S. K. Chowdhury, "Investigations on miniaturized multifrequency microstrip patch antennas for wireless communication applications," *Journal of Electromagnetic Waves and Applications*, Vol. 27, No. 9, 1145–1162, 2013.